Contemporary Mathematics
https://ojs.wiserpub.com/index.php/CM/

Research Article

Neutrosophic Deep Neural Network and Its Application to Soil Microbe Analysis

Rajeshwari Murugesan[1], Nasreen Kausar[2,3], Kaviyarasu Murugan[4], Dragan Pamucar[5*]

[1] Department of Mathematics, Presidency University, Karnataka, 560119, India
[2] Department of Mathematics, Faculty of Arts and Science, Balikesir University, Balikesir, 10145, Turkey
[3] Department of Mathematics, Faculty of Engineering and Natural Sciences, Istinye University, Istanbul, 34396, Turkey
[4] Department of Mathematics, Vel Tech Rangarajan Dr Sagunthala R & D Institute of Science and Technology, Chennai, 600062, India
[5] Sustainability Competence Centre, Széchenyi István University, Egyetem tér 1, Győr, 9026, Hungary
E-mail: pamucar.dragan@sze.hu

Received: 30 June 2025; **Revised:** 2 September 2025; **Accepted:** 5 September 2025

Abstract: An overview of a Neutrosophic Deep Neural Network (NDNN) is given here to illustrate how artificial neural networks and neutrosophic sets can be combined to profit from the comprehensive truth, indeterminate, and falsity degrees known in neutrosophic logic. The investigation details how the NDNN architecture was gradually enriched from its initial and simplest structure, which was a Neutrosophic Neural Network (NNN) with only a one-layer neuron. Next, it progresses to an NNN with one layer and one multi-input neuron, and then becomes even more sophisticated as an NNN with one layer and several multi-input neurons. As a result, the framework concludes with a real NDNN made up of multiple layers, and every layer includes several multi-input neurons. For each network structure, new sets of formulas are given to estimate the parameters of neural networks as neutrosophic triplets for weights and activations. The use of the NDNN in soil microbe processing is demonstrated to prove its usefulness in handling situations with uncertainty and indeterminacy.

Keywords: neutrosophic logic, Neutrosophic Deep Neural Network (NDNN), artificial neural network

MSC: 35R13, 34A07, 34K36

1. Introduction

Soil is fundamental to ecosystem sustainability, serving as the foundation for agriculture, water regulation, nutrient cycling, and biodiversity. At the heart of its functioning lies a rich microbial community that drives essential biochemical processes, ensuring both soil fertility and environmental stability. With rising concerns over climate change and ecological degradation, understanding the dynamics of these microbial populations has become increasingly important. Yet, because soils vary greatly in their composition and exhibit heterogeneous structures, capturing the full complexity of soil-microbe interactions remains a significant scientific challenge.

Traditional modeling methods often struggle to accommodate the uncertainty and imprecision that characterize environmental and biological datasets. Fuzzy logic, however, has proven particularly effective in such contexts. For example, Assimakopoulos et al. [1] combined Geographic Information Systems (GIS) with fuzzy approaches to improve

DOI: https://doi.org/10.37256/cm.7120267652

nitrogen management in agriculture, while Wu et al. [2] employed a Markov chain framework to describe temporal variations in soil structure. Similarly, Tscherko et al. [3] utilized fuzzy classification to better understand changes in biomass activity and enzyme function in grassland ecosystems. Applications also extend to ecological risk assessments, such as Wu et al.'s [4] study on heavy metal contamination.

Beyond methodological advancements, researchers have emphasized the ecological importance of microbial interactions. Traxler and Kolter [5] highlighted how natural products influence microbial behavior and community evolution. Land-use practices, such as forest-grass mosaics, have also been shown to enhance soil quality in diverse landscapes like the Yellow River Delta, as noted by Xia et al. [6]. Together, these findings reinforce the adaptability of fuzzy-based techniques for tackling soil science problems where uncertainty is unavoidable.

Recent progress in computational intelligence has pushed this field even further. Hybrid models, combining fuzzy inference with optimization or evolutionary algorithms, have been developed to address nutrient cycling and phosphorus dynamics (Jha et al. [7]; Jha et al. [8, 9]). Deep learning, with its capacity to detect complex patterns in large datasets, has also been adopted. However, conventional deep neural networks remain limited because they typically process data in rigid, binary terms, making them less effective for uncertain or imprecise systems.

To bridge this gap, researchers have begun merging fuzzy set theory with deep learning architectures, leading to the emergence of Fuzzy Deep Neural Networks (FDNNs). Studies such as those by Deng et al. [10] and Price and Anderson [11] demonstrate how fuzzy integration improves both classification accuracy and interpretability. Comprehensive reviews (Das et al. [12]; Zheng et al. [13]) further emphasize the growing potential of fuzzy deep learning for environmental modeling, where balancing predictive strength with uncertainty awareness is crucial.

Hybrid models continue to gain traction across diverse domains. Wen-Di et al. [14] designed a fuzzy-neural regression framework, showcasing the synergy between learning ability and fuzzy inference. Yazdinejad et al. [15] advanced this direction with an optimized fuzzy deep learning model enhanced by evolutionary algorithms. Applications extend beyond soil science-for instance, Aviso et al. [16] applied fuzzy optimization in sustainable energy systems, while Aghaeipoor et al. [17] demonstrated how fuzzy rules can enhance the interpretability of neural models. Fuzzy evaluation has also been used in environmental risk studies, such as Adeniyi et al.'s [18] holistic assessment of heavy metal contamination in fertilizers.

In soil remediation research, Tian et al. [19] explored the combined role of soil microbes and hyperaccumulator plants (e.g., Sedum alfredii) in detoxifying soils contaminated with heavy metals, highlighting how biological and computational methods together offer new opportunities for sustainable environmental management. Such studies highlight the importance of interdisciplinary approaches that combine biology, environmental science, and computational intelligence. Fuzzy-based deep learning has also been applied in areas such as energy demand prediction, environmental noise reduction, and soil erosion estimation [20–22]. More recent developments by Chen et al. [23] and Pham et al. [24] have focused on deep, ensemble, and hybrid architectures, yielding notable improvements in performance, reliability, and adaptability.

Applications of fuzzy and hybrid systems extend beyond soil science into geohazard mapping and environmental monitoring. Aytop et al. [25] applied the Fuzzy-AHP method for landslide vulnerability assessment, while Fernando et al. [26] employed fuzzy prediction to monitor soil and environmental conditions. Building on this, new neutrosophic-based techniques have shown promising results in agricultural and environmental studies. Alolaiyan et al. [27] developed a linguistic intuitionistic fuzzy approach to enhance soil bioremediation. Sobrinho et al. [28, 29] applied fuzzy-neutrosophic logic to study the effects of elevated CO_2 levels on wheat productivity. Similarly, Atanassov et al. [30] proposed an intuitionistic fuzzy deep neural network framework.

Beyond environmental contexts, neutrosophic methods have been applied to diverse problem domains. Abdalla et al. [31] introduced interval-valued Fermatean neutrosophic super hypersoft sets for prediction and diagnosis in advanced healthcare. Fujita [32] extended Multi-Criteria Decision-Making (MCDM) with hyperfuzzy VIseKriterijumska Optimizacija Kompromisno Resenje (VIKOR) and Decision-Making Trial and Evaluation Laboratory (DEMATEL) methods to address interdependent and vague criteria. Biswas et al. [33] designed a neutrosophic fuzzy decision-making model for strategic site selection under uncertainty, and Basuri et al. [34] proposed a sustainable location framework based on the neutrosophic CRiteria Importance Through Intercriteria Correlation-Complex Proportional Assessment

(CRITIC-COPRAS) approach. Rahaman et al. [35] conducted mathematical analyses of uncertain differential equations with neural uncertainty, contributing to dynamic modeling in indeterminate systems. In financial modeling, Alamin et al. [36] demonstrated the use of neutrosophic fuzzy sets to capture volatility and hesitation in funding data. Fuzzy entropy methodologies to assess the uncertain aspects that bring about corrosion in concrete sewer pipelines situated underground, bringing up some new ideas that have been demonstrated in enhancing the durability of infrastructures built under uncertain conditions [37] Alongside computational approaches, biological processes themselves play a central role in soil remediation and environmental management. Native soil microbes, for example, can reduce toxic and non-essential elements in wastewater-treated soils, thereby lowering contamination risks and contributing to ecosystem recovery [38]. Similarly, plant-microbe partnerships highlight how plants collaborate with specific microbial groups to improve stress tolerance and sustain growth, even under adverse environmental conditions [39].

In parallel with these biological insights, researchers have developed advanced mathematical frameworks to better capture uncertainty in environmental systems. Recent tools such as treesoft sets and neutrosophic sets have been applied to study soil organic matter transformations in urban farming contexts [40], illustrating their potential for tackling complex soil dynamics.

Environmental systems are inherently uncertain due to variations in soil properties, microbial activity, pollutant behavior, and climate fluctuations. Conventional fuzzy logic has long been used to manage this uncertainty by assigning degrees of truth to variables. Intuitionistic fuzzy logic goes a step further by incorporating both membership (truth) and non-membership (falsity) values, with the condition that their sum does not exceed one. While both frameworks are valuable, they remain limited when dealing with contradictory, incomplete, or indeterminate information-scenarios that frequently arise in real-world environmental data.

Neutrosophic logic addresses these shortcomings by introducing a third, independent dimension: indeterminacy. This allows truth, falsity, and uncertainty to be modeled separately, offering a more nuanced and flexible representation of incomplete or conflicting information. Such an approach is particularly powerful in environmental modeling, where hesitation, data gaps, and contradictions are common. By capturing these complexities, neutrosophic logic enables more accurate simulations of soil microbial interactions, pollutant dynamics, and ecological processes.

When integrated with deep learning, this framework gives rise to Neutrosophic Deep Neural Networks (NDNNs). These models hold strong potential for improving predictive accuracy and interpretability, as they combine the pattern recognition power of neural networks with the uncertainty-awareness of neutrosophic logic. As a result, NDNNs can provide a more faithful representation of dynamic soil and environmental processes, ultimately supporting more reliable decision-making in sustainability and remediation efforts.

1.1 *Motivation*

1. Neural networks have problems with uncertainties as well as imprecise data, and this is typical in the application of soil microbes.

2. Classical neural networks cannot handle substantial quantities of indeterminacy and inconsistency due to incompleteness in the real-world information.

3. The Uncertainty of the data in deep learning models can be better represented in the context of Neutrosophic logic.

4. This paper presents a new progressive NDNN framework, which is simple, then multi-layered, and has neutrosophic triplet-based parameterization, and proves its effectiveness through the analysis of soil microbe data.

1.2 *Novelty*

1. The paper presents a methodology for the systematic process of NDNN basic to deep architectures.

2. The neural computation is achieved by integrating neutrosophic values into every layer and level of the neurons.

3. Output estimation under new formulations of neutrosophic modes is derived, such as strongly optimistic to strongly pessimistic.

4. The ability to work in uncertain environments is evidenced in the proposed NDNN, as it is illustrated on soil microbe data and performs better.

1.3 *Research objective*

1. To structure a neural network framework through neutrosophic.
2. To implement and test the model over soil microbe data under uncertain conditions.

1.4 *Structure of the article*

The paper presents a systematic application of neutrosophic set theory to neural networks of varying complexity. Beginning with a single-layer Neutrosophic Neural Network (NNN) containing a single input neuron in Section 3, the study extends the framework to a single-layer network with a multi-input neuron in Section 4. Section 5 further generalizes the concept to multi-layer, multi-input neutrosophic neural networks. For each network type, the research introduces neutrosophic formulations based on five reasoning strategies: strongly optimistic, optimistic, average, pessimistic, and strongly pessimistic. The practical relevance of the proposed NDNN is demonstrated through an application to soil microbial data in Section 6. Subsequent sections include a comparative performance analysis in Section 7, a detailed sensitivity study in Section 8, a discussion of limitations and future research directions in Section 9, and concluding remarks in Section 10.

2. Preliminaries

Definition 1 A NNN is defined as the tuple:

$$\left\langle x_1, x_2, \ldots, x_{n_0} \right\rangle, \left\{ \left\langle y_1^{(r)}, y_2^{(r)}, \ldots, y_{n_r}^{(r)} \right\rangle \middle| 1 \le r \le L \right\}, \left\{ \left\langle \omega_{s,t}^{(r)} \right\rangle \middle| 1 \le s \le n_r, 1 \le t \le n_{r+1}, 0 \le r \le L-1 \right\},$$

$$\left\{ \left\langle \theta_1^{(r)}, \theta_2^{(r)}, \ldots, \theta_{n_r}^{(r)} \right\rangle \middle| 1 \le r \le L \right\}.$$

Where:
• L is the number of layers excluding the input layer;
• n_r is the number of neurons in the r-th layer (n_0 is the number of neurons in the input layer);
• $x_i = \langle \varkappa_i, \varsigma_i, \vartheta_i \rangle$ is a neutrosophic input value, where:
- $\varkappa_i$: degree of truth-membership;
- ς_i: degree of indeterminacy;
- ϑ_i: degree of falsity (non-membership).
• $y_j^{(r)} = \langle \varkappa_j^{(r)}, \varsigma_j^{(r)}, \vartheta_j^{(r)} \rangle$ is the output of the j-th neuron in layer r;
• $\omega_{s,t}^{(r)}$ is the neutrosophic weight from neuron s in layer r to neuron t in layer $r+1$;
• $\theta_j^{(r)}$ is the bias of the j-th neuron in layer r;
• $\phi_j^{(r)}$ is the activation function for the j-th neuron in layer r.

2.1 *Neutrosophic number*

A neutrosophic number is expressed as:

$$N = \langle \varkappa, \varsigma, \vartheta \rangle, \quad \varkappa, \varsigma, \vartheta \in [0, 1], \quad \varkappa + \varsigma + \vartheta \le 3. \tag{1}$$

2.2 *Basic neutrosophic operations*

Let $A = \langle \varkappa_1,\ \varsigma_1,\ \vartheta_1 \rangle$, $B = \langle \varkappa_2,\ \varsigma_2,\ \vartheta_2 \rangle$, then:

- $$A \oplus B = \langle \varkappa_1 + \varkappa_2 - \varkappa_1 \varkappa_2,\ \varsigma_1 \varsigma_2,\ \vartheta_1 \vartheta_2 \rangle . \tag{2}$$

- $$A \vee B = \langle \max(\varkappa_1,\ \varkappa_2),\ \min(\varsigma_1,\ \varsigma_2),\ \min(\vartheta_1,\ \vartheta_2) \rangle . \tag{3}$$

- $$A \odot B = \left\langle \frac{\varkappa_1 + \varkappa_2}{2},\ \frac{\varsigma_1 + \varsigma_2}{2},\ \frac{\vartheta_1 + \vartheta_2}{2} \right\rangle . \tag{4}$$

- $$A \wedge B = \langle \min(\varkappa_1,\ \varkappa_2),\ \max(\varsigma_1,\ \varsigma_2),\ \max(\vartheta_1,\ \vartheta_2) \rangle . \tag{5}$$

- $$A \otimes B = \langle \varkappa_1 \varkappa_2,\ \varsigma_1 + \varsigma_2 - \varsigma_1 \varsigma_2,\ \vartheta_1 + \vartheta_2 - \vartheta_1 \vartheta_2 \rangle . \tag{6}$$

3. NNN with one layer and single-input neuron

Definition 2 We begin with the simplest structure-an NNN with a single layer and a single input neuron as shown in Figure 1.

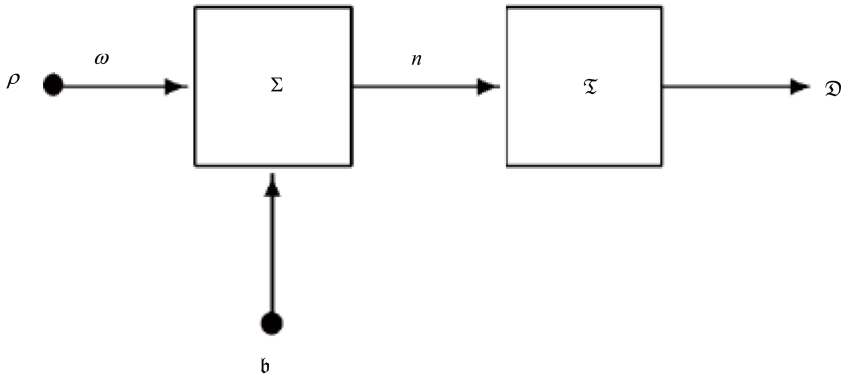

Figure 1. NNN with a single layer and a single input neuron

Let the input to the network be a neutrosophic value:

$$\rho = \langle \varkappa_\rho,\ \varsigma_\rho,\ \vartheta_\rho \rangle, \tag{7}$$

where:

- $\varkappa_\rho$: degree of truth-membership,
- ς_ρ: degree of indeterminacy,
- ϑ_ρ: degree of falsity (non-membership).

The associated weight is also a neutrosophic triplet:

$$\omega = \langle \varkappa_\omega,\ \varsigma_\omega,\ \vartheta_\omega \rangle. \tag{8}$$

The neutrosophic product $\omega \cdot \rho$ can be defined using one of the following strategies:

- Strongly optimistic formula:

$$\omega \cdot \rho = \left\langle 1-(1-\varkappa_\omega)(1-\varkappa_\rho),\ \varsigma_\omega \cdot \varsigma_\rho,\ \vartheta_\omega \cdot \vartheta_\rho \right\rangle. \tag{9}$$

- Optimistic formula:

$$\omega \cdot \rho = \left\langle \max(\varkappa_\omega,\ \varkappa_\rho),\ \min(\varsigma_\omega,\ \varsigma_\rho),\ \min(\vartheta_\omega,\ \vartheta_\rho) \right\rangle. \tag{10}$$

- Average formula:

$$\omega \cdot \rho = \left\langle \frac{\varkappa_\omega + \varkappa_\rho}{2},\ \frac{\varsigma_\omega + \varsigma_\rho}{2},\ \frac{\vartheta_\omega + \vartheta_\rho}{2} \right\rangle. \tag{11}$$

- Pessimistic formula:

$$\omega \cdot \rho = \left\langle \min(\varkappa_\omega,\ \varkappa_\rho),\ \max(\varsigma_\omega,\ \varsigma_\rho),\ \max(\vartheta_\omega,\ \vartheta_\rho) \right\rangle. \tag{12}$$

- Strongly pessimistic formula:

$$\omega \cdot \rho = \left\langle \varkappa_\omega \cdot \varkappa_\rho,\ 1-(1-\varsigma_\omega)(1-\varsigma_\rho),\ 1-(1-\vartheta_\omega)(1-\vartheta_\rho) \right\rangle. \tag{13}$$

The following inequalities justify the naming hierarchy based on the degree:

$$1-(1-\varkappa_\omega)(1-\varkappa_\rho) \geq \max(\varkappa_\omega,\ \varkappa_\rho) \geq \frac{\varkappa_\omega + \varkappa_\rho}{2} \geq \min(\varkappa_\omega,\ \varkappa_\rho) \geq \varkappa_\omega \cdot \varkappa_\rho \tag{14}$$

$$\varsigma_\omega \cdot \varsigma_\rho \leq \min(\varsigma_\omega,\ \varsigma_\rho) \leq \frac{\varsigma_\omega + \varsigma_\rho}{2} \leq \max(\varsigma_\omega,\ \varsigma_\rho) \leq 1 - (1 - \varsigma_\omega)(1 - \varsigma_\rho). \tag{15}$$

Similarly, for the falsity component:

$$\vartheta_\omega \cdot \vartheta_\rho \leq \min(\vartheta_\omega,\ \vartheta_\rho) \leq \frac{\vartheta_\omega + \vartheta_\rho}{2} \leq \max(\vartheta_\omega,\ \vartheta_\rho) \leq 1 - (1 - \vartheta_\omega)(1 - \vartheta_\rho). \tag{16}$$

These expressions reflect increasing or decreasing levels of conservatism in the estimation of the resulting neutrosophic output. The following groups of formulas can likewise be constructed in a similar fashion. Generally, if

$$\kappa,\ \varphi,\ \varpi : [0,\ 1] \times [0,\ 1] \times [0,\ 1] \to [0,\ 1], \tag{17}$$

are two predetermined functions such that, for every $\beth,\ \daleth \in [0,\ 1]$, the condition

$$0 \leq \kappa(\beth,\ \daleth) + \varphi(\beth,\ \daleth) + \varpi(\beth,\ \daleth) \leq 1, \tag{18}$$

is satisfied, then a neutrosophic value n may be represented in the form

$$n = \langle \kappa(\varkappa_\omega,\ \varkappa_\rho),\ \varpi(\varsigma_\omega,\ \varsigma_\rho),\ \varpi(\vartheta_\omega,\ \vartheta_\rho) \rangle, \tag{19}$$

where $\varkappa,\ \varsigma,\ \vartheta$ denote the truth-membership, indeterminacy-membership, and falsity-membership values, respectively, for the components ω and ρ under consideration. The same structural approach applies to subsequent formulas. The output of such an expression is then passed into an aggregation operator Σ (such as a weighted sum or summation function). Additionally, a neutrosophic bias

$$\mathfrak{b} = \langle \varkappa_\mathfrak{b},\ \varsigma_\mathfrak{b},\ \vartheta_\mathfrak{b} \rangle, \tag{20}$$

with each component lying in $[0,\ 1]$, is also included in the aggregation. The final outcome is again expressed in one of the typical neutrosophic forms, integrating the combined influence of input elements and the associated biases. In the context of a neutrosophic neural model, let $n = \langle \varkappa_n,\ \varsigma_n,\ \vartheta_n \rangle$ denote the neutrosophic value of the neuron input, derived from the weights and bias. Several aggregation strategies may be used, depending on the desired degree of optimism or pessimism in the model interpretation:

• Strongly optimistic formula:

$$n = \left\langle 1 - (1 - \varkappa_\omega)(1 - \varkappa_\rho)(1 - \varkappa_\mathfrak{b}),\ \varsigma_\omega \varsigma_\rho \varsigma_\mathfrak{b},\ \vartheta_\omega \vartheta_\rho \vartheta_\mathfrak{b} \right\rangle. \tag{21}$$

• Optimistic formula:

$$n = \left\langle \max(\varkappa_\omega,\ \varkappa_\rho,\ \varkappa_\mathfrak{b}),\ \min(\varsigma_\omega,\ \varsigma_\rho,\ \varsigma_\mathfrak{b}),\ \min(\vartheta_\omega,\ \vartheta_\rho,\ \vartheta_\mathfrak{b}) \right\rangle. \tag{22}$$

• Average formula:

$$n = \left\langle \frac{\varkappa_\omega + \varkappa_\rho + 2\mu_\mathfrak{b}}{4},\ \frac{\varsigma_\omega + \varsigma_\rho + 2\iota_\mathfrak{b}}{4},\ \frac{\vartheta_\omega + \vartheta_\rho + 2\nu_\mathfrak{b}}{4} \right\rangle. \tag{23}$$

• Pessimistic formula:

$$n = \left\langle \min(\varkappa_\omega,\ \varkappa_\rho,\ \varkappa_\mathfrak{b}),\ \max(\varsigma_\omega,\ \varsigma_\rho,\ \varsigma_\mathfrak{b}),\ \max(\vartheta_\omega,\ \vartheta_\rho,\ \vartheta_\mathfrak{b}) \right\rangle. \tag{24}$$

• Strongly pessimistic formula:

$$n = \left\langle \varkappa_\omega \varkappa_\rho \varkappa_\mathfrak{b},\ 1-(1-\varsigma_\omega)(1-\varsigma_\rho)(1-\varsigma_\mathfrak{b},\ 1-(1-\vartheta_\omega)(1-\vartheta_\rho)(1-\vartheta_\mathfrak{b}) \right\rangle. \tag{25}$$

It is important to note that the intermediate neutrosophic parameter $\langle \varkappa_\rho,\ \varsigma_\rho,\ \vartheta_\rho \rangle$ may be computed using a different formula (e.g., the average formula), leading to:

$$n = \left\langle \frac{\varkappa_\omega + \varkappa_\rho + \varkappa_\mathfrak{b}}{3},\ \frac{\varsigma_\omega + \varsigma_\rho + \varsigma_\mathfrak{b}}{3},\ \frac{\vartheta_\omega + \vartheta_\rho + \vartheta_\mathfrak{b}}{3} \right\rangle. \tag{26}$$

The result n is then passed through a transfer function $\mathfrak{T}$, which determines the final neuron output $\mathfrak{O}$.
• For a linear transfer function, the output is:

$$\mathfrak{O} = \mathfrak{T}(n) = \langle \varkappa_n,\ \varsigma_n,\ \vartheta_n \rangle. \tag{27}$$

• For a logical sigmoidal transfer function, the output is:

$$\mathfrak{O} = \frac{1}{1+e^{-n}}, \tag{28}$$

where the input n is treated as a scalar or approximated composite value derived from $\varkappa_n,\ \varsigma_n,\ \vartheta_n$.

We construct the pair

$$\mathfrak{T}_{\text{sigm}}(n) = \left\langle \frac{1}{3}\left(1+\frac{1}{1+e^{-\varkappa_n}}\right),\ \frac{1}{3}\left(1+\frac{1}{1+e^{-\varsigma_n}}\right),\ \frac{1}{3}\left(1+\frac{1}{1+e^{-\vartheta_n}}\right) \right\rangle. \tag{29}$$

Proposition 1 $\mathfrak{T}_{\text{sigm}}$ is a valid Neutrosophic triplet (NP).

Proof. Let the input to the transfer function be a neutrosophic value

$$n = \langle \varkappa_n,\ \varsigma_n,\ \vartheta_n \rangle, \tag{30}$$

where $\varkappa_n$ is the truth-membership, ς_n is the indeterminacy-membership, and ϑ_n is the falsity-membership component, with each in the interval $[0,\ 1]$.

We now verify that each component

$$\left\langle \frac{1}{3}\left(1+\frac{1}{1+e^{-\varkappa_n}}\right),\ \frac{1}{3}\left(1+\frac{1}{1+e^{-\varsigma_n}}\right),\ \frac{1}{3}\left(1+\frac{1}{1+e^{-\vartheta_n}}\right)\right\rangle \in [0,\ 1], \tag{31}$$

and

$$\left\langle \frac{1}{3}\left(1+\frac{1}{1+e^{-\varkappa_n}}\right)+\frac{1}{3}\left(1+\frac{1}{1+e^{-\varsigma_n}}\right)+\frac{1}{3}\left(1+\frac{1}{1+e^{-\vartheta_n}}\right)\right\rangle = \left\langle \frac{1}{3}\left(\frac{1+e^{-\varkappa_n}}{2+e^{-\varkappa_n}}+\frac{1+e^{-\varsigma_n}}{2+e^{-\varsigma_n}}+\frac{1+e^{-\vartheta_n}}{2+e^{-\vartheta_n}}\right)\right\rangle. \tag{32}$$

Combining over a common denominator, and simplifying, and compute the difference:

$$= 12+4e^{-\varkappa_n}+4e^{-\varsigma_n}+4e^{-\vartheta_n}+e^{-\varkappa_n}e^{-\varsigma_n}+e^{-\varsigma_n}e^{-\vartheta_n}+e^{-\varkappa_n}e^{-\vartheta_n} > 0.$$

Each component with proper normalization, $\mathfrak{T}_{\text{sigm}}(n)$ is a valid NP.

4. NNN with one layer and multi-input neuron

Consider a n neuron in Figure 2 that receives as input layers and has values of Neutrosophic Numbers (NNs) defined as:

$$\langle \varkappa_{\rho_1},\ \varsigma_{\rho_1},\ \vartheta_{\rho_1} \rangle, \langle \varkappa_{\rho_2},\ \varsigma_{\rho_2},\ \vartheta_{\rho_2} \rangle, \ldots, \langle \varkappa_{\rho_n},\ \varsigma_{\rho_n},\ \vartheta_{\rho_n} \rangle. \tag{33}$$

The corresponding weight vector consists of neutrosophic coefficients:

$$(\varkappa_{\omega_{j,\,l}},\ \varsigma_{\omega_{j,\,l}},\ \vartheta_{\omega_{j,\,l}}), \quad \text{for } 1 \le j \le n,\ 1 \le l \le n_1. \tag{34}$$

Let the bias term be denoted by the neutrosophic value:

$$(\varkappa_{\mathfrak{b}_l},\ \varsigma_{\mathfrak{b}_l},\ \vartheta_{\mathfrak{b}_l}), \quad \text{for } 1 \le l \le n_1. \tag{35}$$

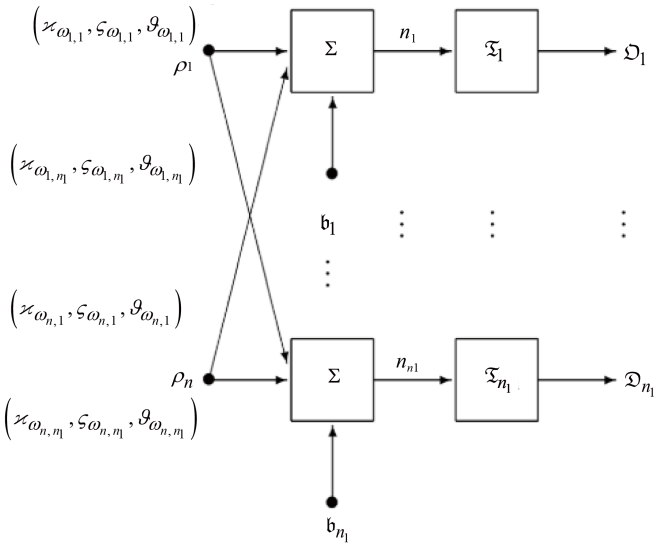

Figure 2. NNN with a one layer and multi-input neuron

Let the aggregated input to the activation function be:

$$z_l = \left\langle \varkappa_{z_l},\ \varsigma_{z_l},\ \vartheta_{z_l} \right\rangle, \quad \text{for } 1 \le l \le n_1. \tag{36}$$

Then, the aggregation formulas for computing z_l are as follows.

4.1 *Strongly optimistic aggregation*

$$z_l = \left\langle 1 - \left(\prod_{i=1}^{n} \left(1 - \varkappa_{\omega_{i,\,l}}\right) (1 - \varkappa_{\rho_i}) \right) (1 - \varkappa_{\mathfrak{b}_l}),\ \left(\prod_{i=1}^{n} \left(\varsigma_{\omega_{i,\,l}} \varsigma_{\rho_i}\right) \right) \varsigma_{\mathfrak{b}_l},\ \left(\prod_{i=1}^{n} \left(\vartheta_{\omega_{i,\,l}} \vartheta_{\rho_i}\right) \right) \vartheta_{\mathfrak{b}_l} \right\rangle. \tag{37}$$

4.2 *Optimistic aggregation*

$$\begin{aligned} z_l = \Bigg\langle & \max\left(\left\{ \max_{i=1}^{n} \left(\varkappa_{\omega_{i,\,l}},\ \varkappa_{\rho_i} \right) \right\} \{\varkappa_{\mathfrak{b}_l}\} \right),\ \min\left(\left\{ \min_{i=1}^{n} \left(\varsigma_{\omega_{i,\,l}},\ \varsigma_{\rho_i} \right) \right\} \{\varsigma_{\mathfrak{b}_l}\} \right), \\ & \min\left(\left\{ \min_{i=1}^{n} \left(\vartheta_{\omega_{i,\,l}},\ \vartheta_{\rho_i} \right) \right\} \{\vartheta_{\mathfrak{b}_l}\} \right) \Bigg\rangle. \end{aligned} \tag{38}$$

4.3 *Average aggregation*

$$z_l = \left\langle \frac{1}{2n} \left(n \cdot \varkappa_{\mathfrak{b}_l} + \sum_{i=1}^{n} \left(\varkappa_{\omega_{i,\,l}} + \varkappa_{\rho_i}\right) \right),\ \frac{1}{2n} \left(n \cdot \varsigma_{\mathfrak{b}_l} + \sum_{i=1}^{n} \left(\varsigma_{\omega_{i,\,l}} + \varsigma_{\rho_i}\right) \right),\ \frac{1}{2n} \left(n \cdot \vartheta_{\mathfrak{b}_l} + \sum_{i=1}^{n} \left(\vartheta_{\omega_{i,\,l}} + \vartheta_{\rho_i}\right) \right) \right\rangle. \tag{39}$$

4.4 *Pessimistic aggregation*

$$z_l = \left\langle \min\left(\left\{\min_{i=1}^{n}\left(\varkappa_{\omega_{i,\,l}},\ \varkappa_{\rho_i}\right)\right\}\{\varkappa_{\mathfrak{b}_\mathfrak{l}}\}\right),\ \max\left(\left\{\max_{i=1}^{n}\left(\varsigma_{\omega_{i,\,l}},\ \varsigma_{\rho_i}\right)\right\}\{\varsigma_{\mathfrak{b}_\mathfrak{l}}\}\right),\right.$$
$$\left.\max\left(\left\{\max_{i=1}^{n}\left(\vartheta_{\omega_{i,\,l}},\ \vartheta_{\rho_i}\right)\right\}\{\vartheta_{\mathfrak{b}_\mathfrak{l}}\}\right).\right. \tag{40}$$

4.5 *Strongly pessimistic aggregation*

$$z_l = \left\langle \left(\prod_{i=1}^{n}\left(\varkappa_{\omega_{i,\,l}}\varkappa_{\rho_i}\right)\right)\varkappa_{\mathfrak{b}_\mathfrak{l}},\ 1-\left(\prod_{i=1}^{n}\left(1-\varsigma_{\omega_{i,\,l}}\right)\left(1-\varsigma_{\rho_i}\right)\right)(1-\varsigma_{\mathfrak{b}_\mathfrak{l}}),\right.$$
$$\left.1-\left(\prod_{i=1}^{n}\left(1-\vartheta_{\omega_{i,\,l}}\right)\left(1-\vartheta_{\rho_i}\right)\right)(1-\vartheta_{\mathfrak{b}_\mathfrak{l}}).\right. \tag{41}$$

5. A NDNN with multiple layers and multi-input neurons

We now consider the most comprehensive case of an NDNN composed of s layers, where each layer consists of several multi-input neurons governed by neutrosophic logic.

Let the first layer follow the structure outlined for a single-layer network, and let each subsequent layer adopt a similar configuration. Each element in these layers is indexed with a superscript x, where $1 \leq x \leq s$. Consider a n neuron that receives as input layers and has values of NNs defined as:

$$\left\langle \varkappa_{\rho_1},\ \varsigma_{\rho_1},\ \vartheta_{\rho_1}\right\rangle, \left\langle \varkappa_{\rho_2},\ \varsigma_{\rho_2},\ \vartheta_{\rho_2}\right\rangle, \ldots, \left\langle \varkappa_{\rho_n},\ \varsigma_{\rho_n},\ \vartheta_{\rho_n}\right\rangle. \tag{42}$$

The corresponding weight vector consists of neutrosophic coefficients:

$$(\varkappa_{\omega_{j,\,l}}, \varsigma_{\omega_{j,\,l}}, \vartheta_{\omega_{j,\,l}}), \quad \text{for } 1 \leq j \leq n,\ 1 \leq l \leq n_1. \tag{43}$$

Let the bias term be denoted by the neutrosophic value:

$$(\varkappa_{\omega_l},\ \varsigma_{\omega_l},\ \vartheta_{\omega_l}), \quad \text{for } 1 \leq l \leq n_1. \tag{44}$$

To enhance predictive performance and decision-making under uncertainty, multiple neutrosophic neural layers are interconnected to form a unified NNN. In this architecture, the output of each layer becomes the input to the subsequent layer, propagating truth, indeterminacy, and falsity values through the network.

This composite structure is typically divided into three principal components:

Input layer: Responsible for receiving external data as neutrosophic values, reflecting the degree of truth, indeterminacy, and falsity of each input.

Hidden layers: One or more intermediate layers that perform the core neutrosophic computations, transforming input signals through weighted combinations and neutrosophic activation functions. These layers capture the underlying uncertainty and conflicting information patterns that define the system's behavior.

Output layer: Tailored to produce the final decision or prediction in the form of neutrosophic values, reflecting nuanced outcomes that preserve partial truth, indeterminacy, and falsity.

When the number of hidden layers exceeds three, the architecture is referred to as a NDNN, leveraging the principles of deep neutrosophic learning. This allows the system to model complex nonlinear relationships, even in the presence of incomplete, inconsistent, or ambiguous data.

Analogous to Sections 3-5, the neutrosophic output

Let the aggregated input to the activation function be:

$$z_l^x = \left\langle \varkappa_{z_l^x},\ \varsigma_{z_l^x},\ \vartheta_{z_l^x} \right\rangle, \quad \text{for } 1 \le l \le n_1,\ 1 \le x \le s. \tag{45}$$

Then, the aggregation formulas for computing z_l^x are as follows.

5.1 *Strongly optimistic aggregation*

$$z_l^x = \left\langle 1 - \left(\prod_{i=1}^{n} \left(1 - \varkappa_{\omega_{i,\,l}^x}\right) \left(1 - \varkappa_{\rho_i^x}\right) \right) \left(1 - \varkappa_{\mathfrak{b}_l^x}\right),\ \left(\prod_{i=1}^{n} \varsigma_{\omega_{i,\,l}^x} \varsigma_{\rho_i^x} \right) \varsigma_{\mathfrak{b}_l^x},\ \left(\prod_{i=1}^{n} \vartheta_{\omega_{i,\,l}^x} \vartheta_{\rho_i^x} \right) \vartheta_{\mathfrak{b}_l^x} \right\rangle. \tag{46}$$

5.2 *Optimistic aggregation*

$$\begin{aligned} z_l^x = \Bigg\langle & \max\left(\left\{ \max_{i=1}^{n} \left(\varkappa_{\omega_{i,\,l}^x},\ \varkappa_{\rho_i^x} \right) \right\} \cup \left\{ \varkappa_{\mathfrak{b}_l^x} \right\} \right),\ \min\left(\left\{ \min_{i=1}^{n} \left(\varsigma_{\omega_{i,\,l}^x},\ \varsigma_{\rho_i^x} \right) \right\} \cup \left\{ \varsigma_{\mathfrak{b}_l^x} \right\} \right), \\ & \left(\left\{ \min_{i=1}^{n} \left(\vartheta_{\omega_{i,\,l}^x},\ \vartheta_{\rho_i^x} \right) \right\} \cup \left\{ \vartheta_{\mathfrak{b}_l^x} \right\} \right). \end{aligned} \tag{47}$$

5.3 *Average aggregation*

$$z_l^x = \left\langle \frac{1}{2n} \left(n \cdot \varkappa_{\mathfrak{b}_l^x} + \sum_{i=1}^{n} \left(\varkappa_{\omega_{i,\,l}^x} + \varkappa_{\rho_i^x} \right) \right),\ \frac{1}{2n} \left(n \cdot \varsigma_{\mathfrak{b}_l^x} + \sum_{i=1}^{n} \left(\varsigma_{\omega_{i,\,l}^x} + \varsigma_{\rho_i^x} \right) \right),\ \frac{1}{2n} \left(n \cdot \vartheta_{\mathfrak{b}_l^x} + \sum_{i=1}^{n} \left(\vartheta_{\omega_{i,\,l}^x} + \vartheta_{\rho_i^x} \right) \right) \right\rangle. \tag{48}$$

5.4 *Pessimistic aggregation*

$$\begin{aligned} z_l^x = \Bigg\langle & \min\left(\left\{ \min_{i=1}^{n} \left(\varkappa_{\omega_{i,\,l}^x},\ \varkappa_{\rho_i^x} \right) \right\} \cup \left\{ \varkappa_{\mathfrak{b}_l^x} \right\} \right),\ \max\left(\left\{ \max_{i=1}^{n} \left(\varsigma_{\omega_{i,\,l}^x},\ \varsigma_{\rho_i^x} \right) \right\} \cup \left\{ \varsigma_{\mathfrak{b}_l^x} \right\} \right), \\ & \max\left(\left\{ \max_{i=1}^{n} \left(\vartheta_{\omega_{i,\,l}^x},\ \vartheta_{\rho_i^x} \right) \right\} \cup \left\{ \vartheta_{\mathfrak{b}_l^x} \right\} \right). \end{aligned} \tag{49}$$

5.5 *Strongly pessimistic aggregation*

$$z_l^x = \left\langle \left(\prod_{i=1}^{n} \varkappa_{\omega_{i,\,l}^x} \varkappa_{\rho_i^x} \right) \varkappa_{\mathfrak{b}_l^x},\ 1 - \left(\prod_{i=1}^{n} \left(1 - \varsigma_{\omega_{i,\,l}^x}\right) \left(1 - \varsigma_{\rho_i^x}\right) \right) \left(1 - \varsigma_{\mathfrak{b}_l^x}\right),\right.$$
$$\left. 1 - \left(\prod_{i=1}^{n} \left(1 - \vartheta_{\omega_{i,\,l}^x}\right) \left(1 - \vartheta_{\rho_i^x}\right) \right) \left(1 - \vartheta_{\mathfrak{b}_l^x}\right) \right\rangle. \tag{50}$$

Training of these different types of NNNs discussed here is performed by a neural network algorithm as shown in Figure 3. The optimization is based on root mean square error to the answer, and the error back-propagation algorithm of keying the sensitivity coefficients throughout the consecutive layers of the network.

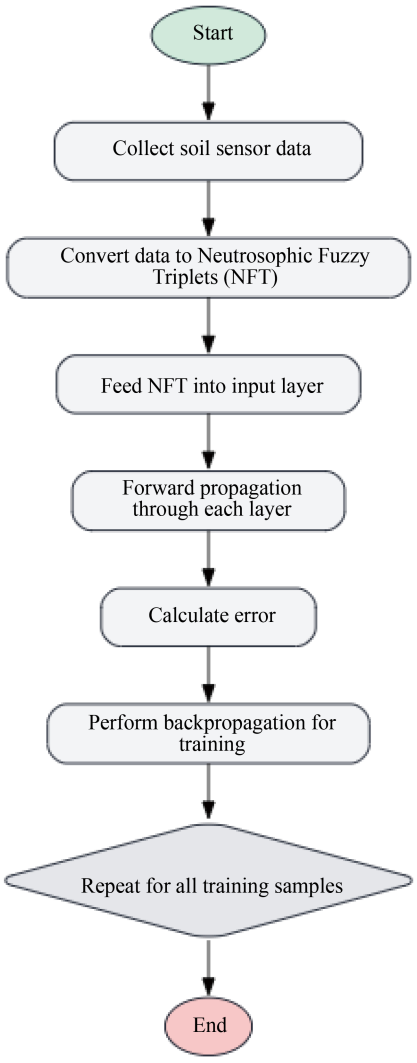

Figure 3. Algorithmic workflow of NDNN-based soil microbe data

In the soil microbe scenario, this model enables assessment of numerous neutrosophic evaluations in consideration of fluctuation in the strength of microbial signals according to the circumstances of uncertainty. Being a representation of biological neuron interactions, these formulations enable one to calculate both downward (pessimistic) and upward (optimistic) limits, determining the repository of microbial reactions. A microbial signal sent to the subsequent layer can die away below a certain threshold and thus stop further propagation, simulating the elimination of microbial activity under unfavourable circumstances. On the other hand, when the optimistic bound of microbial activity is lower than a pre-determined fixed value, this system may be described as a fading case, representing less efficiency in the microbe. Conversely, if the pessimistic bound is greater than some constant, there are two interpretations:

The microbial signal is strong enough to accomplish its functional task in soil bioremediation.

The microbial signal is very strong to the extent that it may overwhelm other microbial functions, effectively forming a blocking phenomenon in the microbial network.

6. NDNN applied to soil microbe data

The current work shows the use of a NDNN model to analyse and forecast soil microbial properties publicly available at Kaggle (https://www.kaggle.com/datasets/isuranga/soil-microbe-dataset). The network accepts input signals with regard to soil parameters like soil moisture content, soil pH, soil organic matter concentration, and nutrient availability in the soil. The process of transformation took place in the following steps:

Data normalization: Min max standardization was applied to each raw variable so that the variables were reduced to $[0,\ 1]$

$$x' = \frac{x - x_{\min}}{x_{\max} - x_{\min}}. \tag{51}$$

Truth-membership calculation: Represents the degree to which the measurement supports a positive outcome or condition of interest. For each normalized attribute x':

$$\varkappa = x'. \tag{52}$$

Indeterminacy-membershipcalculation: Measures the uncertainty caused by the imprecision in measurement, by the missing values, or indecisive indicators. It was calculated:

$$\varsigma = 1 - \exp(-\sigma^2), \tag{53}$$

where σ is the local standard deviation of the attribute within a small neighborhood of samples.

Falsity-membership (ϑ) calculation: Records the degree to which what was measured reflects a negative or conversely opposite result, and is modeled as:

$$\vartheta = 1 - \varkappa. \tag{54}$$

In order to manage it, the data was shifted to the neutrosophic field, where the observations are captured as a triplet.

```
clc; clear; close all;
X = xlsread ('/MATLAB Drive/N. TESTING.xlsx');          % Input file
T = xlsread ('/MATLAB Drive/N TARGET.xlsx');            % Target file
x = x';
T = T';
hiddenLayersizes = [40, 30, 20, 10];                    % You can tune these layer sizes
net = fitnet (hiddenLayersizes, 'trainlm');             % Training function: Levenberg-Marquardt
net.trainParam.epochs       = 1,000;                    % Number of training epochs
net.trainParam.max_fail     = 20;                       % Max validation failures before stop
net.trainParam.min_grad     = 1e-7;                     % Minimum performance gradient
net.trainParam.mu           = 0.001;                    % Initial mu for LM algorithm
net.trainParam.showwindow = true;                       % Show training window
net.divideParam.trainRatio    = 0.70
net.divideParam.valRatio      = 0.15;
net.divideParam.testRatio     = 0.15;
[net, tr] = train (net, X, T);
view (net);                    % opens a window with network architecture
Y_pred = net (x);              % Predict output for all data
figure;
plotregression (T, Y_pred);
title ('Regression Plot: Target vs Predicted');
figure;
plotperform(tr);
mse_error = mse(net, T, Y_pred);
fprintf ('MSE on Full Data: %.4f\n', mse_error);
```

Figure 4. Matlab code for NDNN

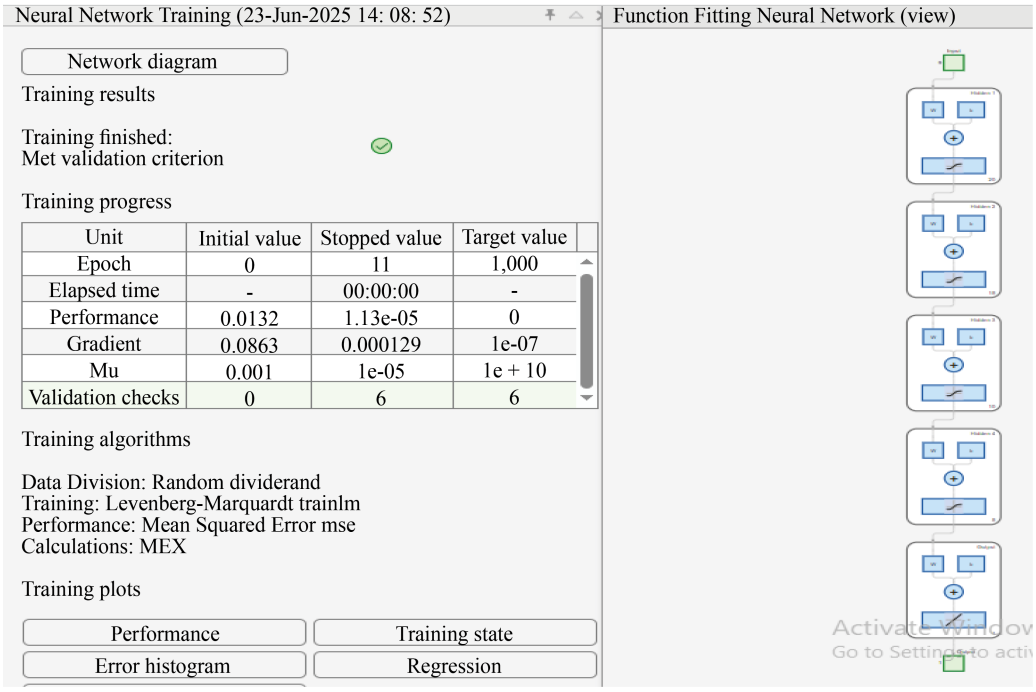

Figure 5. Framework of the developed NDNN model

The neutrosophic version of the data is composed of three variables, which are truth regarding the extent of active microbial existence, indeterminacy concerning the uncertainty in the measurement or environmental variations, and falsity regarding the scope of microbial inactivity or absence. The MATLAB coding for NDNN shown in Figure 4. These three levels are predicted in the network output, which may be used to guide precision agriculture and soil health assessment. A 40-30-20-10-neuron four-layer architecture was utilized to design a network as shown in Figure 5. This design means the modified neutrosophic data is capable of such complicated and nonlinear interactions. Training was made on the Levenberg-Marquardt , and Mean Squared Error (MSE) was used as a measure of performance. The dataset consists of

the first 50 recorded samples, which are randomly partitioned into three as follows: The datasets were randomly partitioned into training (70 percent), validation (20 percent), and test (10 percent). The validation set is an external data set that is not used in the process of weight adjustments in training. It is necessary to mention that the system randomizes the distribution of training/testing/validation data.

Training was terminated at 11 epochs due to the premature stopping criterion that was validated on the performance. The final validation performance had a good level of predictive accuracy with a mean squared error of 2.1×10^{-5}. The error histogram and performance charts verified slight error discrepancies and steady learning behavior in the course of the training and validation phases.

The regression analysis demonstrated strong predictive reliability between the actual and predicted outputs, with a correlation coefficient as shown in Figure 6 follows:

- Training set: $R = 0.99641$
- Validation set: $R = 0.99476$
- Testing set: $R = 0.97257$
- Total sum of data regression: $R = 0.99475$.

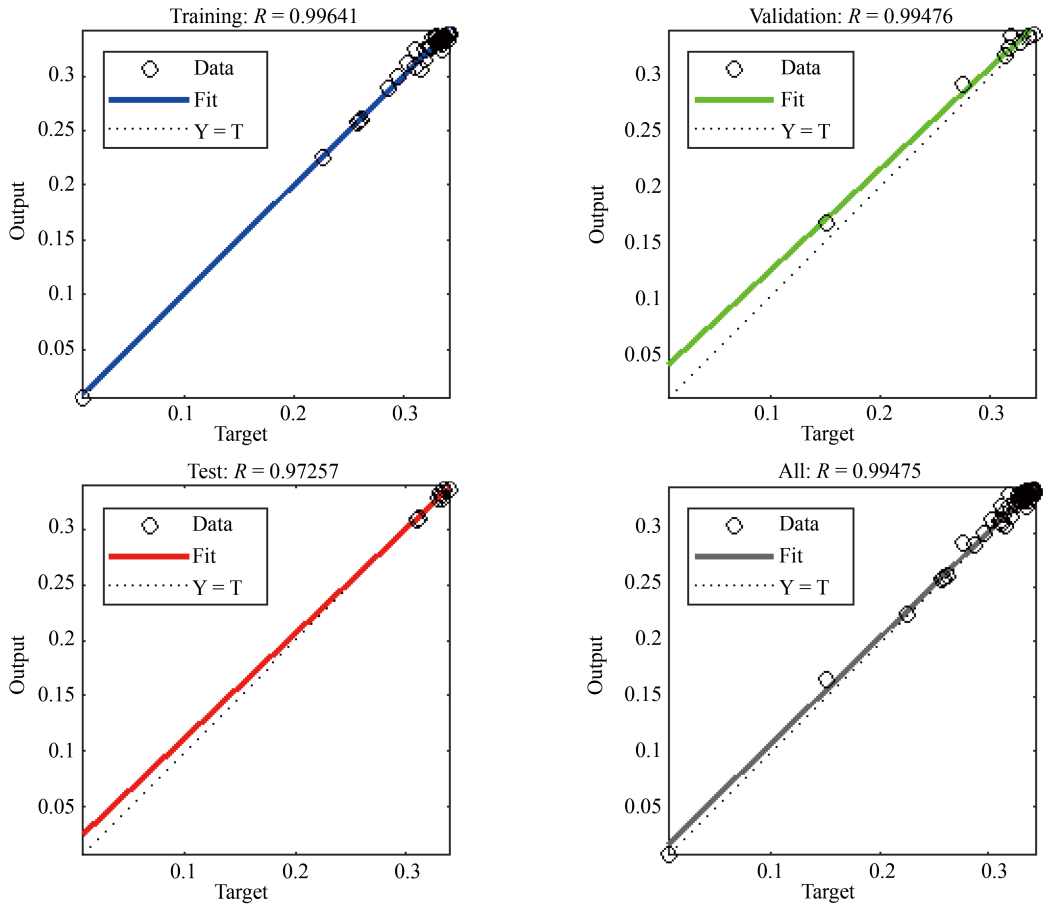

Figure 6. Training, testing, validation, and overall dataset correlation values

These significant R-values in all data divisions testify to the resilience and wide range of generalization of the model. In testing all 50 neutrosophic fuzzy pairs, we achieved the following result: arithmetic mean deviation of 0.2391092 for $\varkappa$, 0.010393 for ς, and 0.2391097 for ϑ.

This NDNN framework can be applied in future projects with bigger datasets, i.e. long time monitoring of soil microbial population with various crop rotations or varying climate change scenarios. The active microbial biomass can be quantified as the estimated truth value, the falsity value can be used to locate microbial dormancy zones, and the indeterminacy value can be used to identify areas where additional sampling is necessary as a result of indeterminacy or the lack of environmental data.

7. Comparative analysis

The proposed NDNN was evaluated through comparative studies focusing on accuracy, robustness, computational efficiency, and sensitivity. Across training, testing, and validation datasets, the NDNN consistently achieved higher correlation coefficients than traditional Feedforward Neural Networks (FNN), conventional Deep Neural Networks (DNN), and Neutrosophic Fuzzy Neural Networks (NFNN). Its ability to simultaneously process truth, indeterminacy, and falsity enabled superior handling of uncertainty. The model exhibited faster convergence and greater interpretability, albeit with a slightly higher computational cost. Additionally, a five-level estimation strategy-comprising strongly optimistic, optimistic, average, pessimistic, and strongly pessimistic modes-was introduced, allowing adaptive interpretation under varying uncertainty levels. This capability, absent in the baseline models, highlights the NDNN's effectiveness in predicting soil microbial dynamics in complex environments.

8. Sensitivity analysis

Evaluation of the performance of the NDNN is essential, particularly when handling soil microbe data characterized by inherent uncertainty and indeterminacy. To test the sensitivity and strength of the model, a systematic sensitivity analysis is required to understand the dependencies of changes in the input of neutrosophic values, which comprise truth, indeterminacy, and falsity. elements stimulate a general predictive performance. In this analysis, there is:

• Evaluate NDNN with five different neutrosophic decision rules (strongly optimistic, optimistic, average, pessimistic, strongly pessimistic) to conclude how the model reacts to various attitudes of uncertainties against soil microbe data.

• Training, testing, and validation datasets to assess the impact of fluctuation in neutrosophic input on the accuracy of predictions.

• Investigating the effects of network depth and neuron count on model robustness and computational efficiency, providing guidance for designing NDNNs capable of handling imprecise soil microbe data effectively.

9. Limitations and future outlook

The current study has certain limitations, primarily stemming from the high complexity of the stratified neutrosophic model, which can make real-time implementation challenging in environments with limited computational resources. The model is also highly dependent on the quality and accuracy of input data, such as soil microbial measurements, which may affect its reliability. Additionally, its applicability to other domains remains uncertain and requires further empirical validation. Future work should focus on optimizing parameter tuning, developing lightweight versions of the model suitable for edge-device deployment, and integrating Explainable AI techniques to enhance interpretability and practical usability in diverse applications.

10. Conclusion

This study demonstrates the systematic development of a NDNN, beginning with a single-layer, single-input neuron network. The methodology is then extended to a single-layer network with a multi-input neuron, followed by a one-layer

architecture comprising multiple multi-input neurons, and finally culminating in a multi-layered deep neural network with several multi-input neurons. The research uniquely introduces five reasoning paradigms-strongly optimistic, optimistic, average, pessimistic, and strongly pessimistic-for evaluating the summation outputs of each network type. The proposed neutrosophic deep neural network has been successfully applied to real-world soil microbe data, highlighting its practical applicability. Beyond this, the model shows potential for broader scientific applications wherever sensitive neutrosophic evaluation of information is required.

Conflict of interest

The authors declare no competing financial interest.

References

[1] Assimakopoulos JH, Kalivas DP, Kollias VJ. A GIS-based fuzzy classification for mapping the agricultural soils for N-fertilizers use. *Science of the Total Environment*. 2003; 309(1-3): 19-33.

[2] Wu K, Nunan N, Crawford JW, Young IM, Ritz K. An efficient Markov chain model for the simulation of heterogeneous soil structure. *Soil Science Society of America Journal*. 2004; 68(2): 346-351.

[3] Tscherko D, Kandeler E, Bárdossy A. Fuzzy classification of microbial biomass and enzyme activities in grassland soils. *Soil Biology and Biochemistry*. 2007; 39(7): 1799-1808.

[4] Wu YG, Xu YN, Hu SH, Zhang JH, Li JG. Ecological risk assessment of heavy metals in contaminated soil based on engineering fuzzy set theory. *Advanced Materials Research*. 2010; 113: 815-818.

[5] Traxler MF, Kolter R. Natural products in soil microbe interactions and evolution. *Natural Product Reports*. 2015; 32(7): 956-970.

[6] Xia J, Ren J, Zhang S, Wang Y, Fang Y. Forest and grass composite patterns improve the soil quality in the coastal saline-alkali land of the Yellow River Delta, China. *Geoderma*. 2019; 349: 25-35.

[7] Jha SK, Ahmad Z. Soil microbial dynamics modeling in fluctuating ecological situations by using subtractive clustering and fuzzy rule-based inference systems. *Computer Modeling in Engineering & Sciences*. 2017; 113(4): 443-459.

[8] Jha SK, Ahmad Z, Crowley DE. Fuzzy inference for soil microbial dynamics modeling in fluctuating ecological situations. *Journal of Intelligent & Fuzzy Systems*. 2018; 35(2): 1399-1406.

[9] Jha SK, Ahmad Z, Crowley DE. Fuzzy-genetic approaches for estimation of microbial rock phosphate solubilization in sandy clay loam textured soil. *Computers and Electronics in Agriculture*. 2018; 150: 125-133.

[10] Deng Y, Ren Z, Kong Y, Bao F, Dai Q. A hierarchical fused fuzzy deep neural network for data classification. *IEEE Transactions on Fuzzy Systems*. 2016; 25(4): 1006-1012.

[11] Price SR, Anderson DT. Introducing fuzzy layers for deep learning. In: *2019 IEEE International Conference on Fuzzy Systems (FUZZ-IEEE)*. New Orleans, LA, USA: IEEE; 2019. p.1-6.

[12] Das R, Sen S, Maulik U. A survey on fuzzy deep neural networks. *ACM Computing Surveys*. 2020; 53(3): 1-25.

[13] Zheng Y, Xu Z, Wang X. The fusion of deep learning and fuzzy systems: A state-of-the-art survey. *IEEE Transactions on Fuzzy Systems*. 2021; 30(8): 2783-2799.

[14] Wen-Di Z, De-Wang C, Yong-Qiang Z, Yun-Hu H. Deep neural fuzzy system algorithm and its regression application. *Acta Automatica Sinica*. 2020; 46(11): 2350-2358.

[15] Yazdinejad A, Dehghantanha A, Parizi RM, Epiphaniou G. An optimized fuzzy deep learning model for data classification based on NSGA-II. *Neurocomputing*. 2023; 522: 116-128.

[16] Aviso KB, Sy CL, Tan RR. Fuzzy optimization of direct and indirect biomass co-firing in power plants. *Chemical Engineering Transactions*. 2019; 76: 55-60.

[17] Aghaeipoor F, Sabokrou M, Fernández A. Fuzzy rule-based explainer systems for deep neural networks: From local explainability to global understanding. *IEEE Transactions on Fuzzy Systems*. 2023; 31(9): 3069-3080.

[18] Adeniyi H, Akorede S, Opeyemi M, Adebayo I, Adelabu A, Michael S. Towards achieving food security in Nigeria: A fuzzy comprehensive assessment of heavy metals contamination in organic fertilizers. *Current Research in Agricultural Sciences*. 2021; 8(2): 110-127.

[19] Tian Z, Li G, Tang W, Zhu Q, Li X, Du C, et al. Role of Sedum alfredii and soil microbes in the remediation of ultra-high content heavy metals contaminated soil. *Agriculture, Ecosystems & Environment*. 2022; 339: 108090.
[20] Islam MR, Jaafar WZW, Hin LS, Osman N, Hossain A, Mohd NS. Development of an intelligent system based on ANFIS model for predicting soil erosion. *Environmental Earth Sciences*. 2018; 77: 1-15.
[21] Sideratos G, Ikonomopoulos A, Hatziargyriou ND. A novel fuzzy-based ensemble model for load forecasting using hybrid deep neural networks. *Electric Power Systems Research*. 2020; 178: 106025.
[22] Han HG, Zhang HJ, Qiao JF. Robust deep neural network using fuzzy denoising autoencoder. *International Journal of Fuzzy Systems*. 2020; 22(4): 1356-1375.
[23] Chen C, Cao Y, Chen X, Wu D, Xiong C, Huang J. A fused deep fuzzy neural network controller and its application to pneumatic flexible joint. *IEEE/ASME Transactions on Mechatronics*. 2023; 28(6): 3214-3225.
[24] Pham P, Nguyen LT, Nguyen NT, Kozma R, Vo B. A hierarchical fused fuzzy deep neural network with heterogeneous network embedding for recommendation. *Information Sciences*. 2023; 620: 105-124.
[25] Aytop H, Saygin F, Dengtz O, Alaboz P. Determination of landslide susceptibility with the Fuzzy-Analytical Hierarchical Process-Andırın Example. *Proceedings*. 2023; 84. Availavle from: https://doi.org/10.1007/s10661-023-12100-0.
[26] Fernando BS, Malik MRM, Putra FGD, Sukma SH, Darmawan MDM, Octavia N, et al. Prediction fuzzy implementation in monitoring system based on humidity, soil quality, and environmental conditions. *Journal of Applied Science, Technology & Humanities*. 2024; 1(3): 227-241.
[27] Alolaiyan H, Hayat M, Shuaib U, Razaq A, Salman MA, Xin Q. Optimizing bioremediation techniques for soil decontamination in a linguistic intuitionistic fuzzy framework. *Scientific Reports*. 2024; 14(1): 15979.
[28] Sobrinho RL, Oliveira BR, Zuffo AM, Teixeira Filho M, Marques Filho AC, Zoz T, et al. A fuzzy yield model of the wheat inoculated with Rhizophagus irregularis under future climate elevated CO_2. *Scientific Reports*. 2024; 14(1): 15979.
[29] Sobrinho RL, de Oliveira BR, Zuffo AM, Zoz T, Okla MK, Alaraidh IA, et al. Modeling wheat productivity under elevated CO_2 using fuzzy logic and mycorrhizal inoculation. *BMC Plant Biology*. 2025; 25(1): 1-13.
[30] Atanassov K, Sotirov S, Pencheva T. Intuitionistic fuzzy deep neural network. *Mathematics*. 2023; 11(3): 716.
[31] Abdalla MEM, Uzair A, Ishtiaq A, Tahir M, Kamran M. Algebraic structures and practical implications of interval-valued fermatean neutrosophic super hyperSoft sets in healthcare. *Spectrum of Operational Research*. 2025; 2(1): 199-218.
[32] Fujita T. The hyperfuzzy VIKOR and hyperfuzzy DEMATEL methods for multi-criteria decision-making. *Spectrum of Decision Making and Applications*. 2025; 3(1): 292-315.
[33] Biswas A, Gazi KH, Bhaduri P, Mondal SP. Neutrosophic fuzzy decision-making framework for site selection. *Journal of Decision Analytics and Intelligent Computing*. 2024; 4(1): 187-215.
[34] Basuri T, Gazi KH, Bhaduri P, Das SG, Mondal SP. Decision-analytics-based sustainable location problem-neutrosophic CRITIC-COPRAS assessment model. *Management Science Advances*. 2025; 2(1): 19-58.
[35] Rahaman M, Mondal SP, Ahmad S, Gazi KH, Ghosh A. Study of the system of uncertain linear differential equations under neutrosophic sense of uncertainty. *Spectrum of Engineering and Management Sciences*. 2025; 3(1): 93-109.
[36] Alamin A, Biswas A, Gazi KH, Sankar SPM. Modelling with neutrosophic fuzzy sets for financial applications in discrete system. *Spectrum of Engineering and Management Sciences*. 2024; 2(1): 263-280.
[37] Wani TI, Rallapalli S, Singhal A, Robert D, Kodikara J, Pramanik BK, et al. Compounded fuzzy entropy-based derivation of uncertain critical factors causing corrosion in buried concrete sewer pipeline. *NPJ Clean Water*. 2025; 8(1): 36.
[38] Kekana IKJ, Kgopa PM, Munjonji L. Bioremediation of non-essential toxic elements using indigenous microbes in soil following irrigation with treated wastewater. *Applied Sciences*. 2025; 15(5): 2299.
[39] Liu S, Wu J, Cheng Z, Wang H, Jin Z, Zhang X, et al. Microbe-mediated stress resistance in plants: the roles played by core and stress-specific microbiota. *Microbiome*. 2025; 13(1): 111.
[40] Vizuete PC. A study using treesoft set and neutrosophic sets on possible soil organic transformations in urban agriculture systems. *International Journal of Neutrosophic Science*. 2025; 25(1): 1.